The DIRECT Project: Influence of Blending on the Cepheid Distance Scale. I. Cepheids in M31

B. J. Mochejska[1]

Copernicus Astronomical Center, 00-716 Warszawa, Bartycka 18
e-mail: mochejsk@camk.edu.pl

L. M. Macri, D. D. Sasselov[2], K. Z. Stanek[3]

Harvard-Smithsonian Center for Astrophysics, 60 Garden St., Cambridge, MA 02138
e-mail: lmacri, dsasselov, kstanek@cfa.harvard.edu

ABSTRACT

We investigate the influence of blending on the Cepheid distance scale. Blending is the close association of a Cepheid with one or more intrinsically luminous stars. High-resolution *HST* images are compared to our ground-based data, obtained as part of the DIRECT project, for a sample of 22 Cepheids in the M31 galaxy. The average (median) V-band flux contribution from luminous companions which are not resolved on the ground-based images is about 19% (12%) of the flux of the Cepheid. This is a large effect − at the 10% level for distances. The current Cepheid distance estimates to M31 are all ground-based, and are thus affected (underestimated). We discuss indirect methods to find which Cepheids are blended, e.g. by the use of well-sampled light curves in at least two optical bands. More generally, our ground-based resolution in M31 corresponds to the *HST* resolution at about 10 Mpc. Blending leads to systematically low distances in the observed galaxies, and therefore to systematically high estimates of H_0; we discuss the issue and the implications.

1.   Introduction

As the number of extragalactic Cepheids discovered with *HST* continues to increase and the value of H_0 is sought from distances based on these variables (e.g. Saha et al. 1999; Mould et al. 2000), it becomes even more important to understand various possible systematic errors which could affect the extragalactic distance scale. Currently, the most important systematic is a bias in the distance to the Large Magellanic Cloud, which provides the zero-point calibration for the Cepheid distance scale. The LMC distance is very likely significantly shorter than usually assumed

---

[1]Visiting Student, Harvard-Smithsonian Center for Astrophysics

[2]Alfred P. Sloan Foundation Fellow

[3]Also N. Copernicus Astronomical Center, Bartycka 18, Warszawa PL-00-716, Poland

(e.g. Udalski 1998; Stanek et al. 2000), but it still might be considered uncertain at the $\sim 10\%$ percent level (e.g. Jha et al. 1999). Another possible systematic, the metallicity dependence of the Cepheid Period-Luminosity (PL) relation, is also very much an open issue, with the empirical determinations ranging from 0 to $-0.4\ mag\ dex^{-1}$ (Freedman & Madore 1990; Sasselov et al. 1997; Kochanek 1997; Kennicutt et al. 1998).

In this paper we investigate a much neglected systematic, that of the influence of blended stellar images on the derived Cepheid distances. Although Cepheids are very bright, $M_V \sim -4$ at a period of 10 $days$, their images when viewed in distant galaxies are likely to be blended with other nearby, relatively bright stars. We define $blending$ as the close projected association of a Cepheid with one or more intrinsically luminous stars, which can not be detected within the observed point-spread function (PSF) by the photometric analysis (e.g., DAOPHOT, DoPHOT). Such blended stars are mostly other young stars which are physically associated − from actual binary and multiple systems to companions which are not gravitationally bound to the Cepheid. Blending is thus a phenomenon different from $crowding$ or $confusion\ noise$; the latter occurs in stellar fields with a crowded and complex background due to the random superposition of stars of different luminosity. In this paper we are concerned with blending due to wide unbound systems. Binary Cepheid companions are well studied (Evans 1992), and do not contribute enough flux to affect Cepheid distances (Madore 1977), due to the obvious constraints of coeval stellar evolution. On the other hand, the association of Cepheids with other luminous stars in wide unbound systems is an unsolved problem in general. While such association, i.e. a strong star-star correlation function, is expected and common to young stars (Harris & Zaritsky 1999), the specific case for Cepheids is unknown. Studies in our Galaxy are very difficult due to the small sample and existing results, though tantalizing, are inconclusive (Evans & Udalski 1994). This could explain the relative neglect of this issue in recent years, but blending had been of concern for early studies of Magellanic Cloud Cepheids (DeYoreo & Karp 1979; Pel, van Genderen & Lub 1981), because even faint B-star blends affect the optical colors of a Cepheid significantly.

We investigate the effects of stellar blending on the Cepheid distance scale by studying two Local Group spiral galaxies, M31 and M33. In this paper we concentrate on M31 (Andromeda Galaxy), located at approximately $R_{M31} = 780\ kpc$ (e.g. Holland 1998; Stanek & Garnavich 1998) from us. As part of the DIRECT project (e.g. Kaluzny et al. 1998; Stanek et al. 1998) we have collected for this galaxy an extensive data set, finding among other variables 206 Cepheids. We identify some of these Cepheids on archival HST-WFPC2 images and compare them to our ground-based data to estimate the impact of blending on our photometry, taking advantage of their superior resolution – the FWHM on the WFPC2 camera corresponds to $\sim 0.4\ pc$ at the distance of M31, compared to $\sim 5\ pc$ for the ground-based data. The average FWHM on the DIRECT project ground-based images of M31 is about $1.5''$, or $\sim 5\ pc$, which corresponds to the HST-WFPC2 resolution of $0.1''$ for a galaxy at a distance of 10 Mpc. Any luminous star (or several of them) in a volume of that cross section through the disk (at the inclination of the galaxy) could be indistinguishable from the Cepheid and would contribute to its measured flux.

As Cepheids are relatively young stars, they reside strictly in the midplanes of the disks of spiral galaxies.

The archival *HST*-WFPC2 study of M31 Cepheids from our project DIRECT was undertaken to improve our distance determination to the galaxy. The preliminary indirect (via LMC) Cepheid distance we obtained (Kaluzny et al. 1998; Sasselov et al. 1998) was practically the same as the Cepheid distance by Freedman & Madore (1990) of $R_{M31} = 770 \pm 25\ kpc$. Our findings of blending now indicate that these distance estimates should be corrected upward.

We describe the ground-based and *HST* data and the applied reduction procedures in Section 2. In Section 3 we discuss the task of identifying Cepheids on *HST* WFPC2 images. In Section 4 we present the blending catalog of Cepheids and discuss it in Section 5. In Section 6 we describe the effect of blending on the light and color curves of Cepheids and how these curves can be used to detect blends. In Section 7 we discuss the effectiveness of some of the blend analysis methods encountered in the literature. The concluding remarks are to be found in Section 8.

2.   Observations and Data Reduction

2.1.   Ground-based Data

The ground-based data were obtained as part of the DIRECT project between September 1996 and October 1997 during 95 full/partial nights on the F. L. Whipple Observatory 1.2 m telescope and 36 full nights on the Michigan-Dartmouth-MIT 1.3 m telescope. Six $11' \times 11'$ fields with a scale of 0.32 $''$/pixel were monitored: four of them (A–D) concentrated on the rich spiral arm in the northeast part of M31, one (E) close to the bulge of M31 and one (F) containing the giant star formation region known as NGC 206. Fields A–D and F have been reduced and the BVI photometry of Cepheid variables published in Stanek et al. 1998 (hereafter, Paper II), Kaluzny et al. 1998 (Paper I), Stanek et al. 1999 (Paper III), Kaluzny et al. 1999 (Paper IV) and Mochejska et al. 1999 (Paper V), respectively. The applied reduction, calibration and variable selection procedures are discussed therein, particularly in Paper I, where full details are provided. A total of 206 Cepheids were found: 43 in field A, 38 in B, 35 in C, 38 in D and 52 in field F.

2.2.   HST data

The archival *HST*-WFPC2 data used in this paper were retrieved from the Hubble Data Archive. We selected images overlapping our M31 ground-based data, taken in filters F336W (roughly U), F439W, F450W ($\sim B$), F555W, F606W ($\sim V$) and F814W ($\sim I$). The pixel scales of the Wide Field (WF) and Planetary Camera (PC) chips are 0.0996 and 0.0455 $''$/pixel, respectively. The full list of exposures is provided in Table 1, along with the proposal ID, dataset name, equatorial coordinates of the frame centers, filter and exposure time information.

Table 1. THE FULL LIST OF *HST* IMAGES CONTAINING DIRECT CEPHEIDS

Proposal ID	Dataset Name	$\alpha_{J2000.0}$	$\delta_{J2000.0}$	Filter	Exp. Time (s)
5911	U2Y20103T	00 44 44.17	41 27 33.88	F336W	400
5911	U2Y20105T	00 44 44.23	41 27 33.86	F439W	160
5911	U2Y20106T	00 44 44.23	41 27 33.86	F555W	140
5911	U2Y20203T	00 44 49.28	41 28 59.04	F336W	400
5911	U2Y20205T	00 44 49.34	41 28 59.03	F439W	160
5911	U2Y20206T	00 44 49.34	41 28 59.03	F555W	140
5911	U2Y20303T	00 44 57.57	41 30 51.68	F336W	400
5911	U2Y20305T	00 44 57.63	41 30 51.65	F439W	160
5911	U2Y20306T	00 44 57.63	41 30 51.65	F555W	140
5911	U2Y20403T	00 45 09.20	41 34 30.56	F336W	400
5911	U2Y20405T	00 45 09.25	41 34 30.72	F439W	160
5911	U2Y20406T	00 45 09.25	41 34 30.72	F555W	140
5911	U2Y20503T	00 45 11.89	41 36 56.86	F336W	400
5911	U2Y20505T	00 45 11.95	41 36 57.02	F439W	160
5911	U2Y20506T	00 45 11.95	41 36 57.02	F555W	140
6038	U2YE0603T	00 44 51.22	41 30 03.72	F555W	160
6038	U2YE0605T	00 44 51.22	41 30 03.72	F439W	600
6038	U2YE060BT	00 44 51.22	41 30 03.72	F336W	900
6038	U2YE060DT	00 44 51.22	41 30 03.72	F336W	900
5237	U2AB0101T	00 40 29.40	40 43 58.28	F555W	200
5237	U2AB0102T	00 40 29.40	40 43 58.28	F555W	200
5237	U2AB0103T	00 40 29.40	40 43 58.28	F814W	200
5237	U2AB0104T	00 40 29.40	40 43 58.28	F814W	200
5237	U2AB0105T	00 40 29.40	40 43 58.28	F336W	600
5237	U2AB0106T	00 40 29.40	40 43 58.28	F336W	600
5494	U2G20701T	00 40 33.17	40 45 38.97	F606W	350
8059	U4WOAH02R	00 40 10.11	40 46 08.91	F606W	400
8059	U4WOAH04R	00 40 10.11	40 46 08.91	F450W	600
8059	U4WOAH05R	00 40 10.11	40 46 08.91	F814W	100
8059	U4WOAH06R	00 40 10.11	40 46 08.91	F814W	300
8061	U4X1OF01R	00 40 10.11	40 46 08.91	F606W	400

The data we obtained had already passed through the standard preliminary processing and calibration procedures prior to its placement in the Archive. The standard pipeline calibration is fully described in the *HST* Data Handbook.

The first two steps in our reduction procedure were to mark the bad pixels on the images and to compensate for the fact that pixels on the edges and corners of the CCD receive fewer photons due to the geometric distortion in the WFPC2 optics. For each image a mask was created from the data quality file retrieved from the Archive and a vignetting mask generated by Stetson (1998) and then used to mark bad pixels and vignetted regions. To restore the integrity of the flux measurements the images were multiplied by a pixel-area map, originally created by Holtzman et al. (1995) and renormalized to the median pixel area on each chip by Stetson (1998). These tasks were accomplished under IRAF[4].

In the next step of the reduction procedure pairs (or multiplets) of images were selected, taken in the same filters, having identical center coordinates as well as similar exposure times. The **crrej** task under IRAF was used to combine the images and remove cosmic rays. When multiple images for a given field were not available, single images were used for photometry.

The photometry was extracted by means of the DAOPHOT/ALLSTAR package (Stetson 1987, 1992). Stars were identified using the FIND subroutine and aperture photometry was done on them with the PHOT subroutine. We used the point-spread functions (PSF) derived individually for each filter and chip of the WFPC2 camera, kindly provided to us by P. B. Stetson (private communication) to obtain the ALLSTAR profile photometry. After the initial ALLSTAR run, FIND was ran again on the star subtracted images, to identify stars that were missed on the first pass. Aperture photometry was obtained for them with PHOT, followed by profile photometry with ALLSTAR. The two star lists were merged and used as input to ALLSTAR to obtain the final photometry.

It should be noted that the *HST* photometry has not been calibrated to any standard system and therefore instrumental magnitudes are used throughout this paper. This has, however, no bearing on the results presented in this paper, since they are strictly based on differential photometry.

3. The Identification of DIRECT Cepheids in *HST* Data

The preliminary identification of DIRECT Cepheids on the *HST* frames was accomplished by a visual comparison of the *HST* data matched via World Coordinate System (WCS) information to

---

[4]IRAF is distributed by the National Optical Astronomy Observatories, which are operated by the Association of Universities for Research in Astronomy, Inc., under cooperative agreement with the NSF.
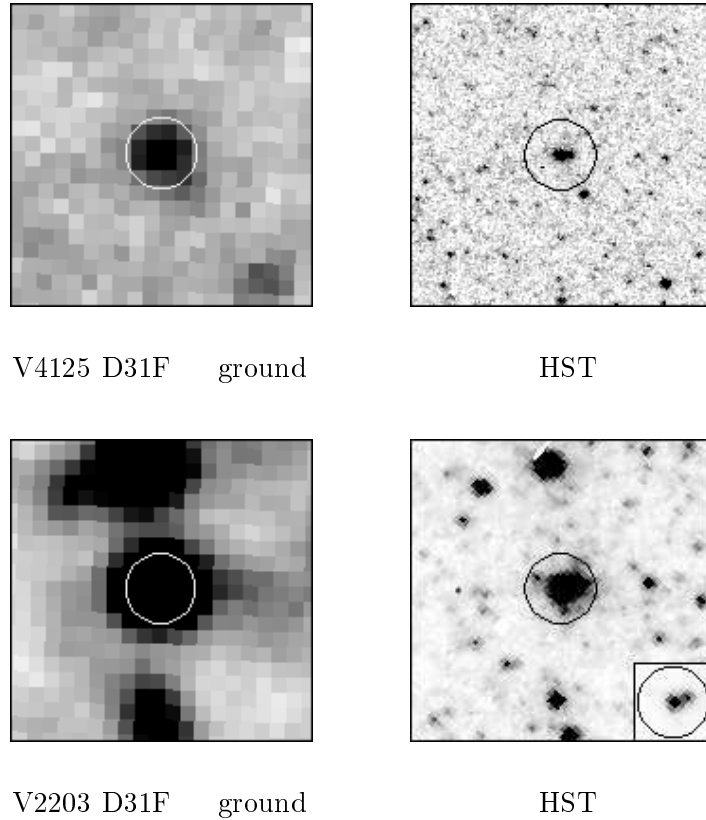
Fig. 1.— A comparison of ground-based and *HST* data for two Cepheids: V4125 D31F and V2203 D31F. The images plotted in the left panels are taken from the *V* template. The circles, centered on the Cepheids, have a radius of 0.75″. The inset in the lower right panel has different IRAF z-scale limits to show the two blended stars separately.

our ground-based *V* template image for each field, using SAOimage ds9[5]. The WCS information for the ground-based template image header was obtained with a program written by Mink (1997; 1999) by matching stars from the image to the USNO A2.0 Catalog stars (Monet et al. 1996). We have matched a total of 22 Cepheids to *HST* data: six in our field B, four in C (two of them on two different overlapping fields) and 12 in field F (one found on two different fields). This constitutes ∼ 18% of the 125 Cepheids in fields B, C and F.

In some cases, when a Cepheid which appeared to be a single star on the *V* template was resolved into multiple stars on an *HST* image, it was difficult to distinguish which star was the Cepheid on the basis of the template image alone. Two such cases are shown in Figure 1. The images plotted in the left panels are taken from the *V* template, created by averaging together two

---

[5]SAOimage ds9 was developed under a grant from NASA's Applied Information System Research Program (NAG5-3996), with support from the Chandra Science Center (NAS8-39073)

images with the best seeing (FWHM $\sim 1''$). The image in the upper right panel was taken with the PC chip of the WFPC2 camera while the one in the lower right panel comes from a WF chip. The inset has different IRAF z-scale limits to show the two blended stars separately. The circles, centered on the Cepheids, have a radius of $0.75''$. The Cepheid V4125 D31F is shown in the upper panels of the Figure 1. On the ground-based template it appears as a single star, while on the PC chip it is resolved into two objects, one 3 magnitudes dimmer than the other. A third star appears below and to the right, just outside the circle, fainter by almost 2 magnitudes from the brighter component of the doublet. That star was not identified on the ground-based template image, but after subtracting the Cepheid a brighter spot is visible at that location. The lower panels show the case of V2203 D31F, where the Cepheid, appearing as a single star on the ground V template image, is resolved by HST into two stars, differing by one magnitude in brightness.

To help confirm the Cepheid nature of the selected objects, instrumental color-magnitude diagrams (CMDs) were constructed from HST data, whenever photometry in two bands was available. A few representative CMDs are shown in Figure 2, $(v_{F555W}, v_{F555W} - i_{F814W})$ in the left panels and $(v_{F555W}, b_{F439W} - v_{F555W})$ in the right panels. The Cepheids are denoted by circles and their companions by squares. Stars from the same chip are plotted in the background for reference. The upper left panel shows a case where there is a substantial contribution of flux from a red giant companion $((\frac{f}{f_C})_V = 34\%, (\frac{f}{f_C})_I = 67\%)$ which is seen at a distance of $0.2''$ from the Cepheid V1893 D31F. The other companion is a blue star at a distance of $0.4''$ which appears to be located at the red edge of the main sequence (also in the $v_{F555W}, u_{F336W} - v_{F555W}$ CMD which is not shown). The lower left panel presents a case where the Cepheid V2203 D31F has a luminous blue main sequence companion with $(\frac{f}{f_C})_V = 40\%$ and $(\frac{f}{f_C})_I = 17\%$ which are separated by $0.3''$. The upper right panel shows the Cepheid V7184 D31B with two blue main sequence companions, the more luminous one, located $0.4''$ away, contributing 45% as much light as the Cepheid in the B band and 23% in V. A typical situation where none of the companions (in this case one) had b-band photometry (see Table 2) is illustrated in the lower right panel of Figure 2, where the Cepheid V4954 D31B is shown.

4. M31 Blending Catalog

4.1. The Catalog

The criterion for blending was determined empirically, by careful examination of ground-based and HST data for the same Cepheids. We consider a star to be blended with the Cepheid if it is located at a distance of less than $0.75''$ from it and is not detected by DAOPHOT in our ground-based images. The choice of maximum distance was motivated by the typical full width at half maximum (FWHM) in our ground-based images ($\sim 1.5''$).

Due to the relatively small number of Cepheids having HST data, it was deemed worthwhile to examine them on the HST images in detail to see whether all of the companions had been
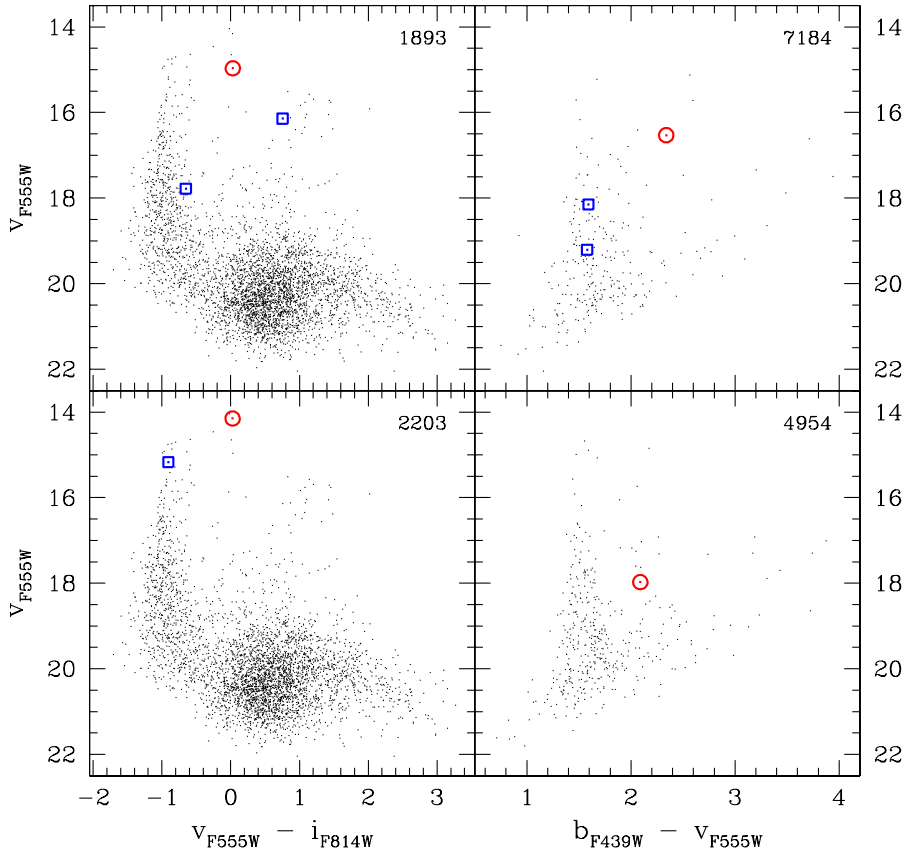
Fig. 2.— Selected color-magnitude diagrams for Cepheids and their companions within 0.75″ based on *HST* data. The Cepheids are denoted by circles and their companions by squares. Stars from the same chip are plotted in the background.

identified by DAOPHOT and to check for the possibility of false detections (cosmic rays in case of single images, bad columns, etc.). In the latter case the object was removed from the list. Not much could be done in the former case, although that proved not to be a problem and only in a few of the 55 examined images there were very faint companions which eluded detection. It must be noted that the FWHM of the PSF on the WF chip is of the order of 1 pixel and so the probability of the detection of a faint star may depend on the way its light is distributed over the pixels. One exception, however, is V1893 D31F, which DAOPHOT failed to recognize as a star on one of the single F606W filter images, along with its companion 2 pixels (0.2″) away. No problem was encountered on the other three combined images.

We estimate that our data is fairly complete for companions contributing at least 4% of the flux of the Cepheid in the V band (filters F555W and F606W). We have used this somewhat arbitrary cutoff in evaluating the sum S_F of all flux contributions in filter F normalized to the flux of the Cepheid:

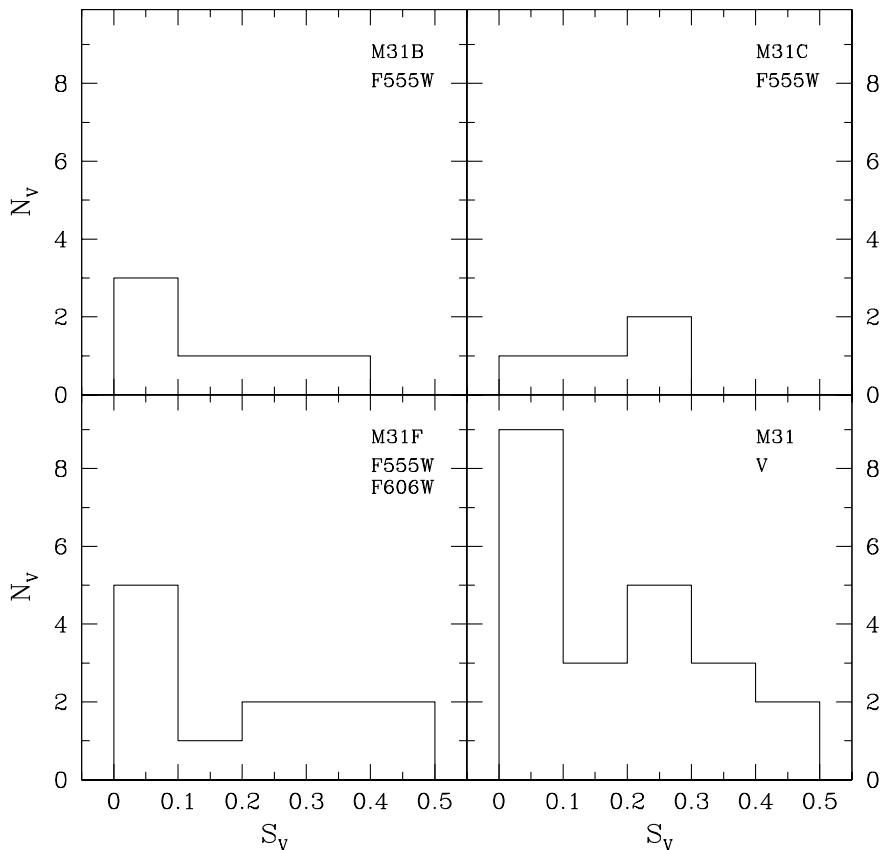$$S_F = \sum_{i=1}^{N_F} \frac{f_i}{f_C} \tag{1}$$

Fig. 3.— A histogram showing the number of Cepheids N_V as a function of $S_V = \sum_{i=1}^{N_F} \frac{f_i}{f_C}$, the sum of flux contributions from its companions in the V band (filters F555W and F606W), normalized to the flux of the Cepheid. The upper left and right panels and the lower left panel are for fields B, C and F, respectively; the lower right panel is the combined data.

where f_i is the flux of the i-th companion, f_C the flux of the Cepheid on the *HST* image and N_F the total number of companions. In Table 2 we present the results for each of the 22 Cepheids found in the *HST* images: the name, the mean V, I and B magnitudes taken from Papers II, III and V, the number of companions N_F and their total flux contribution S_F in the V, I, B and U bands respectively. Unless noted otherwise, the V, as in N_V and S_V, refers to filter F555W, I to F814W, B to F439W and U to F336W. For the two Cepheids identified on two *HST* images, the average values of S_F are listed.

The catalog of Cepheid blending in M31 is illustrated in the following two figures. Figure 3 shows a histogram of the number of Cepheids N_V as a function of S_V (Eq. 1), the sum of flux contributions from its companions in the V band (filters F555W and F606W), normalized to the flux of the Cepheid. The upper left and right panels and the lower left panel show the histograms for fields B, C and F, respectively. In the lower right panel the combined data is shown. The width of each bin is 0.1 and the first one starts at 0. For further discussion on Figure 3 see §5.

Table 2.   THE CEPHEID BLENDING CATALOG

Name	$\langle V \rangle$	$\langle I \rangle$	$\langle B \rangle$	N_V	S_V	N_I	S_I	N_B	S_B	N_U	S_U
V7184 D31B	19.15	18.45	$\cdots$	3	0.40		$\cdots$	2	0.62	3	2.55
V6379 D31B	20.65	19.39	$\cdots$	3	0.27		$\cdots$	0	0.00		$\cdots$
V7209 D31B	20.07	19.14	$\cdots$	1	0.12		$\cdots$	0	0.00	1	0.96
V5646 D31B	20.90	19.51	$\cdots$	1	0.05		$\cdots$	0	0.00		$\cdots$
V4954 D31B	20.86	19.98	$\cdots$	1	0.10		$\cdots$	0	0.00	0	0.00
V6872 D31B	21.60	20.62	$\cdots$	1	0.05		$\cdots$	0	0.00	0	0.00
V14487 D31C	19.95	18.95	20.75	2	0.12		$\cdots$	0	0.00	1	0.60
V13705 D31C	21.50	19.98	22.83	0	0.00		$\cdots$		$\cdots$		$\cdots$
V14661 D31C	21.39	19.70	22.76	2	0.30		$\cdots$	0	0.00		$\cdots$
V14361 D31C	21.21	19.32	22.36	3	0.27		$\cdots$	0	0.00		$\cdots$
V4125 D31F	20.46	19.63	21.11	1	0.06	3	0.25		$\cdots$	0	0.00
V3289 D31F	20.89	19.76	20.77	2	0.11	3	0.27		$\cdots$	1	0.53
V3550 D31F	20.55	19.85	21.03	2	0.47	0	0.00		$\cdots$	1	6.33
V1893 D31F	18.79	17.47	19.54	2	0.41	1	0.66		$\cdots$	1	0.33
V2203 D31F	17.94	17.17	18.32	1	0.39	1	0.17		$\cdots$	3	2.88
V3860 D31F	21.24	19.65	22.08	0	0.00	3	0.63		$\cdots$	0	0.00
V3441 D31F	21.28	20.52	21.18	2	0.26[1]		$\cdots$		$\cdots$		$\cdots$
V2320 D31F	20.27	19.54	20.60	0	0.00[1]		$\cdots$		$\cdots$		$\cdots$
V1633 D31F	21.30	19.85	$\cdots$	1	0.10[1]		$\cdots$		$\cdots$		$\cdots$
V1599 D31F	20.94	19.86	21.78	4	0.34[1]		$\cdots$		$\cdots$		$\cdots$
V1549 D31F	20.72	19.68	21.49	4	0.28[1]		$\cdots$		$\cdots$		$\cdots$
V7074 D31F	20.78	19.70	21.51	0	0.00[1]	0	0.00	0	0.00[2]		$\cdots$

Note. — [1] results obtained in the F606W filter
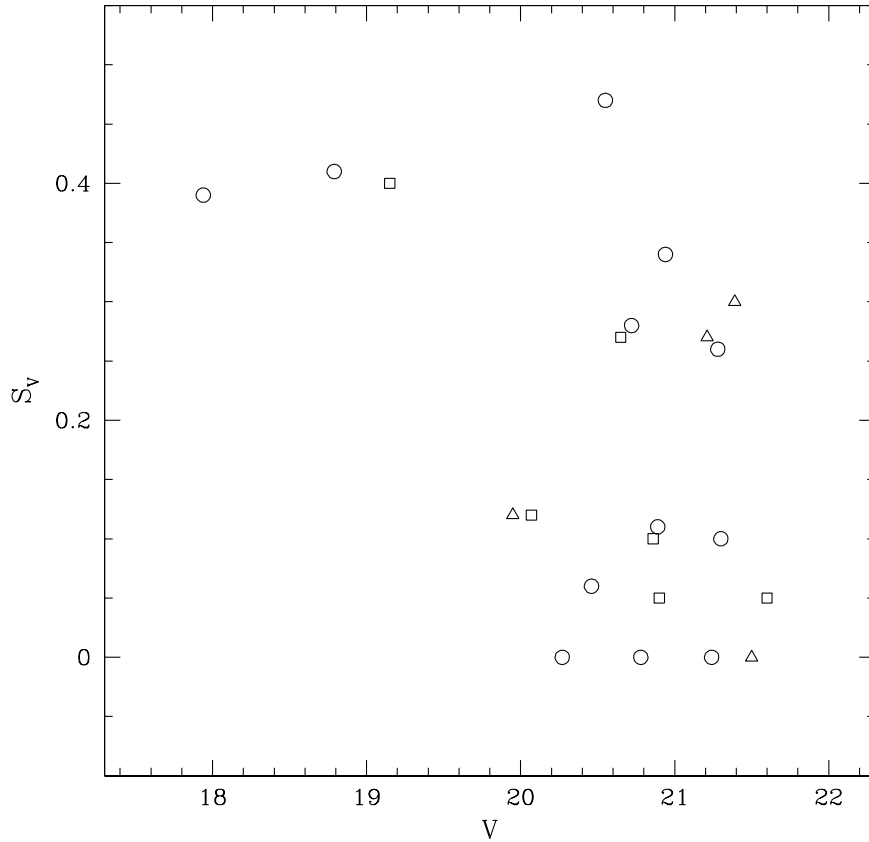[2] results obtained in the F450W filter

Fig. 4.— Cepheid blending is not a function of magnitude, *i.e.*, luminosity, at the same distance in M31. A diagram of the flux contribution from companions $S_V = \sum_{i=1}^{N_F} \frac{f_i}{f_C}$ as a function of the V magnitude of the Cepheid obtained from ground-based data for all 22 DIRECT Cepheids present in *HST* data. Field B Cepheids are denoted by squares, field C by triangles and field F by circles.

A diagram showing the flux contribution from companions S_V as a function of the V magnitude of the Cepheid obtained from ground-based data (Papers II, III and V) is presented in Figure 4. Field B Cepheids are denoted by squares, field C by triangles and field F by circles.

4.2. The Blended Cepheids and their Environments

The first step in using the derived blending is to see what is the effect on the Cepheid period-luminosity (P-L) relation. Figure 5 illustrates the influence of blending on the location of the Cepheids on the P-L diagram. The solid circles show the original locations of the Cepheids, based on their mean V magnitudes obtained from the ground-based data. The arrows illustrate the shift in V when the effects of blending are taken into account. It has to be kept in mind that neither the differential reddening in M31 nor the random-phase nature of the *HST* data have been accounted for, thus there is significant scatter in the diagram. However, the direction and the
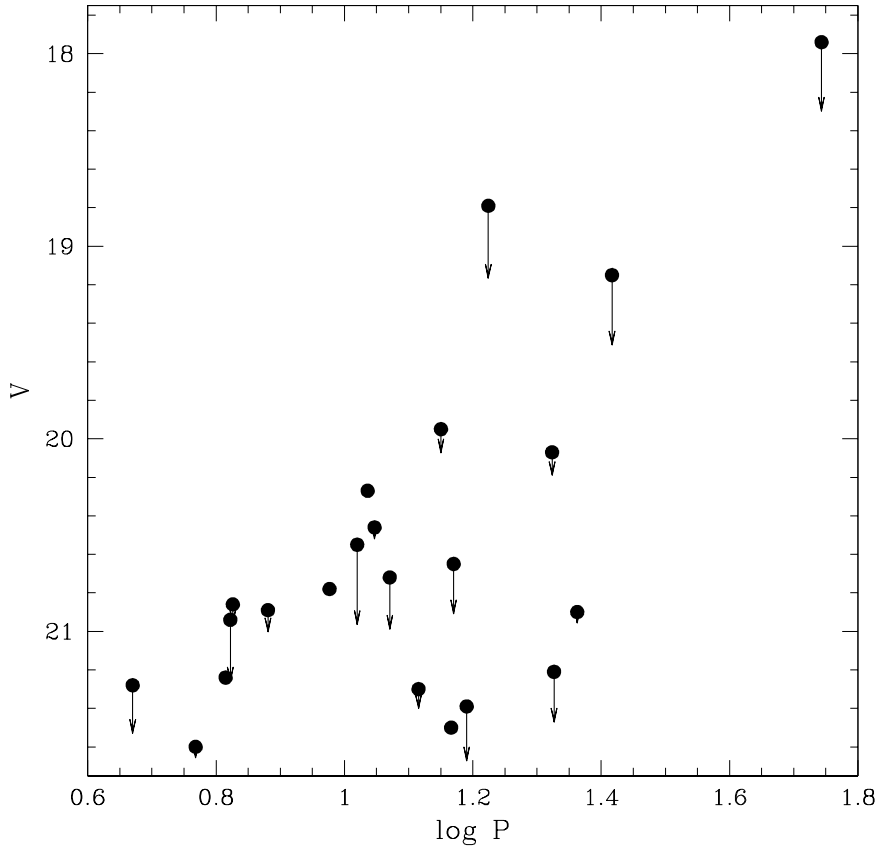
Fig. 5.— The $\log P$ vs. V diagram for the 22 Cepheids found in *HST* data (reddening and the random-phase nature of the *HST* data are not accounted for). The arrows illustrate the shift in V when the effects of blending are taken into account. The effect is significant, but it is not a function of period.

magnitude of the effect is obvious.

A pattern in the spatial distribution of Cepheid blending in M31 could show us a correlation between blending and crowding. We find no such correlation – Cepheids in environments of different surface brightness show roughly the same frequency and amount of blending, thus distinguishing the phenomenon of blending from crowding. In Figure 6 the blending parameter S_V is plotted as a function of the surface brightness around the Cepheid for which it was determined. The surface brightness was taken to be the mode within a 20 pixel radius on the DIRECT template frames. We used a bin width of 1 ADU for the histogram to compute the value of the mode, smoothed with a flat-topped rectangular kernel (boxcar) filter, 11 units in length. After correcting for the sky level, the instrumental surface brightness values were converted to mag/□″using 12-17 fairly bright isolated reference stars with known standard magnitudes by means of the following formula:

$$SB \, [\text{mag}/\square''] = m_{ref} + 2.5 \log(s^2 I_{ref}/I_{SB})$$

where I_{ref} and m_{ref} are the flux in ADU/□ pixel and the corresponding magnitude of the reference
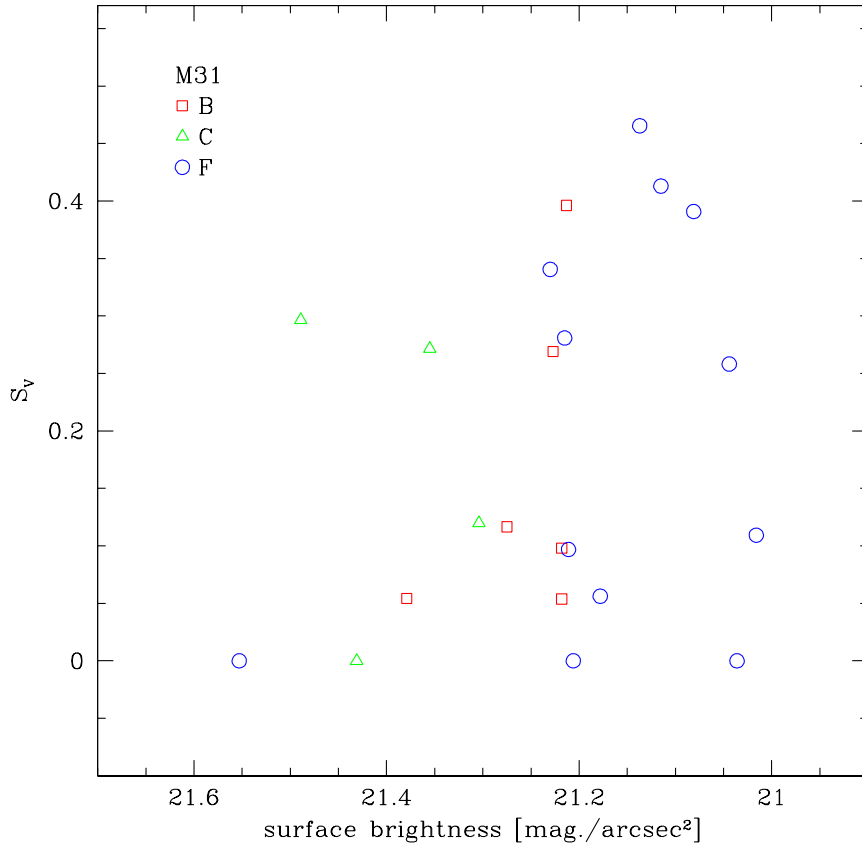
Fig. 6.— Blending S_V as a function of the surface brightness around the M31 Cepheids on the ground-based templates. Field B Cepheids are denoted by squares, field C by triangles and field F by circles. Cepheid blending does not seem to correlate with surface brightness.

star, I_{SB} is the surface brightness expressed in ADU/$\square$ pixel and s is the pixel scale of the chip. The rms scatter around the value of the average ranged from 0.025 to 0.061 mag/$\square''$.

In order to give these numbers some perspective, we have computed surface brightness around Cepheids in two galaxies which straddle their range, NGC 2541 and NGC 4535 (Fig. 7). We find that the Cepheids we discover in M31 reside in environments of surface brightness typical of spiral galaxies, despite the high inclination of M31. The *HST* data for these galaxies, observed as part of the HST Key Project on the Extragalactic Distance Scale (Ferrarese et al. 1998, Macri et al. 1999), were obtained from the Hubble Data Archive. Since we were unable to estimate the sky level for those images, we tried to choose epochs where the sky level would be the lowest. We chose the 1995 Nov 20 epoch for NGC 3541 and the 1996 May 24 epoch for NGC 4535. The surface brightness values were computed using the same method as for our M31 Cepheids and were re-expressed in units of mag/$\square''$ using the zeropoints provided in the HST Data Handbook.
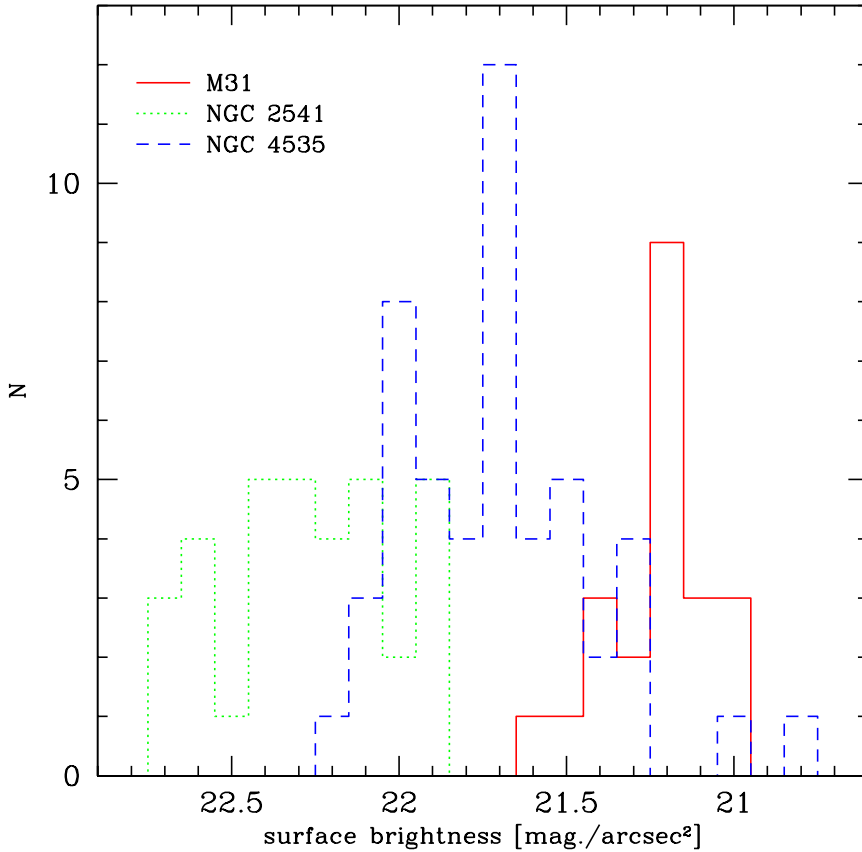
Fig. 7.— The surface brightness around Cepheids in M31, NGC 4535 and NGC 2541. The Cepheids that we observe in M31 do not reside in anomalously high surface brightness areas.

5.   Discussion of Blending Properties

Before attempting to draw any far-reaching conclusions from Figs. 3-7 or the catalog itself (Tab. 2), we must stress that they are based on a fairly small sample of Cepheids and therefore subject to statistical uncertainties. An illustration of this effect is the small number of counts in the second bin of the combined histogram (Fig. 3), compared to the third and, especially, the first bin, which could be an artifact of small number statistics. An encouraging fact is that the distributions in separate fields, especially B and F, appear to be similar to a substantial degree in their overall shape and spanned range of S_V. In the combined histogram there is a decreasing trend in the number of cases N_V with increasing flux contribution from blending, S_V.

The diagram in Fig. 4 conveys some of the information contained in the previous figure – a lack of cases with $0.12 \leq S_V \leq 0.23$ is readily apparent, which, as mentioned above, is believed to result from the fairly small size of the sample. If we attribute the gap to statistical effects, then Cepheids fainter than $V \sim 20$ appear to populate a wide range of S_V, from 0 up to approximately 0.35, with one object at $S_V \sim 0.47$. Furthermore, it is observed that in none of the fields do Cepheids show a tendency to favor any particular value of S_V, as also apparent from Figure 3.

Another striking feature of the diagram is that all of the three Cepheids brighter than $V \sim 20$ have $S_V \sim 0.4$, although it has to be emphasized that this sample is much too small to draw any definite conclusions. One possible explanation may be ventured, however, which may hold true in these particular cases, but does not have to be the rule for the whole population of bright Cepheids. The most luminous Cepheids are the most massive ones and, hence, the youngest. The group or association of stars in which they had formed will have had less time to disperse. This may manifest itself in a somewhat higher spatial density of stars and thus would increase the probability of blending.

Figure 6 shows the blending parameter S_V of the M31 Cepheids as a function of the local surface brightness. As there is a gap at $S_V \sim 0.2$, the separation into blended ($S_V > 0.25$) and unblended Cepheids ($S_V < 0.15$) is readily discernible in the diagram. No correlation between the blending parameter S_V and the underlying surface brightness is apparent.

To put the surface brightness values around the M31 Cepheids into perspective, we plot the surface brightness values computed for the NGC 4535 and NGC 2541 Cepheids (Fig. 7). The range of surface brightness of NGC 2541 falls below the range of our M31 Cepheids. There is a 26% overlap between the NGC 4535 and M31 data – 13 out of the 50 Cepheids in NGC 4535 are located in regions with surface brightness in the range covered by our M31 Cepheids.

It should be kept in mind that our sample may also be affected to some extent by selection effects: for example, 11 of our Cepheids are located in the vicinity of NGC 206, the giant star-forming region in M31. Additionally, M31 is observed at a rather high inclination angle, which is not a typical situation for most galaxies searched for Cepheids. An opportunity to study the effects of blending with a larger sample of ~ 100 Cepheids, in a more face-on system, will present itself in the next paper on Cepheids in M33 (Mochejska et al. 2000). We will also discuss there the influence of blending on the observed colors of Cepheids.

6.   Blending and the Light Curves

The luminosity variations through the pulsation cycle of a Cepheid seen in the optical are due primarily to changes in temperature. The monochromatic surface brightness changes with temperature and is additionally quite dependent on wavelength. Of course, the Cepheid also expands and contracts − its area varies. This contributes to the total light variation in a wavelength independent way. The radius variation in a typical Cepheid is out of phase by about $90°$ with respect to the surface brightness variation. Therefore a comparison between color (proxy for temperature variation) and magnitude (proxy for luminosity variation, due to *both* radius and temperature change) would produce a loop in the CMD plane.

These loops, i.e. the tight correlation between color and luminosity, have had a limited use in the past as part of the Cepheid PLC calibration (Fernie 1964), or to transform away the temperature-induced variation (Madore 1985; Moffett & Barnes 1986). The characterization of

Cepheid companions had been traditionally done by using the similar loops in the color-color plane of optical bands (Stobie 1970). The color-color loop arises from the phase shift introduced between the pair of color-magnitude relations when a companion of different temperature (i.e. color) is added. Blue or red companions distort the color-color loops in very different and quantifiable ways (Madore 1977; DeYoreo & Karp 1979) and can be very effective in deriving the amount of and color of contamination in a Cepheids flux.

In order to understand the wavelength-dependent effect of a blue or red companion on the light curves (and loops) of a Cepheid, one should bear in mind that the contaminant flux is most prominent during the minimum in the Cepheid lightcurve, and gradually becomes insignificant as the Cepheid brightens up during its cycle. The addition of a *red companion* to the flux of a Cepheid has the following effects on its optical light curves: (1) the light curve exhibits a flatter minimum (due to the added flux); (2) the color curve has a deeper minimum (due to the added red flux); and (3) the asymmetry in the color curve decreases. The addition of a *blue companion* to the flux of a Cepheid has the following effects on its optical light curves: (1) the light curve exhibits a flatter minimum (as above); (2) the color curve has a flatter minimum (due to the added blue flux); and (3) the asymmetry in the color curve increases.

A typical example is the Cepheid V7184 D31B (Paper I), which has blue blends (Table 2) and whose CM loop is shown in Fig. 8. The effect on its loop is predictable given the above discussion: as the Cepheid fades and becomes naturally redder, the added constant blue flux of the blends becomes more prominent and diverts the lower part of the loop to the blue (left in Fig. 8). This diversion could result eventually in a complete reversion of the naturally clockwise trajectory of the loop. If the data is incomplete (there are two gaps in the light curves of V7184), the blue blending is still detectable by the steeper slope of the loop.

These changes on the color-magnitude plane, together with a fit of the mean colors of the Cepheid to extinction laws, can be a powerful means to find and characterize blended Cepheids in a sample like our DIRECT project one. The necessary requirement is − good, well-sampled light curves in at least two bands. Therefore we were able to find blended Cepheids like V7184 in M31B and exclude them from our analysis without the benefit of *HST* images, but just using our light curves (Paper I). However, the technique is limited to the cases with strongest blending – a nonlinear fitting routine by Rebel (1998) applied to the M31B data still did not detect 2/3 of the blended Cepheids we found in this paper. In other words, the naive technique of visual inspection for ”flat-bottom” light curves is completely inadequate for detecting 10%-20% Cepheid blending, which is dominating our findings in M31.

7. Blend Analysis by the HST Key Project in the Galaxy NGC 2541

The influence of blending has been largely neglected in many recent galaxy distance determinations based on Cepheids. Few attempts have been made to deal with this problem. On
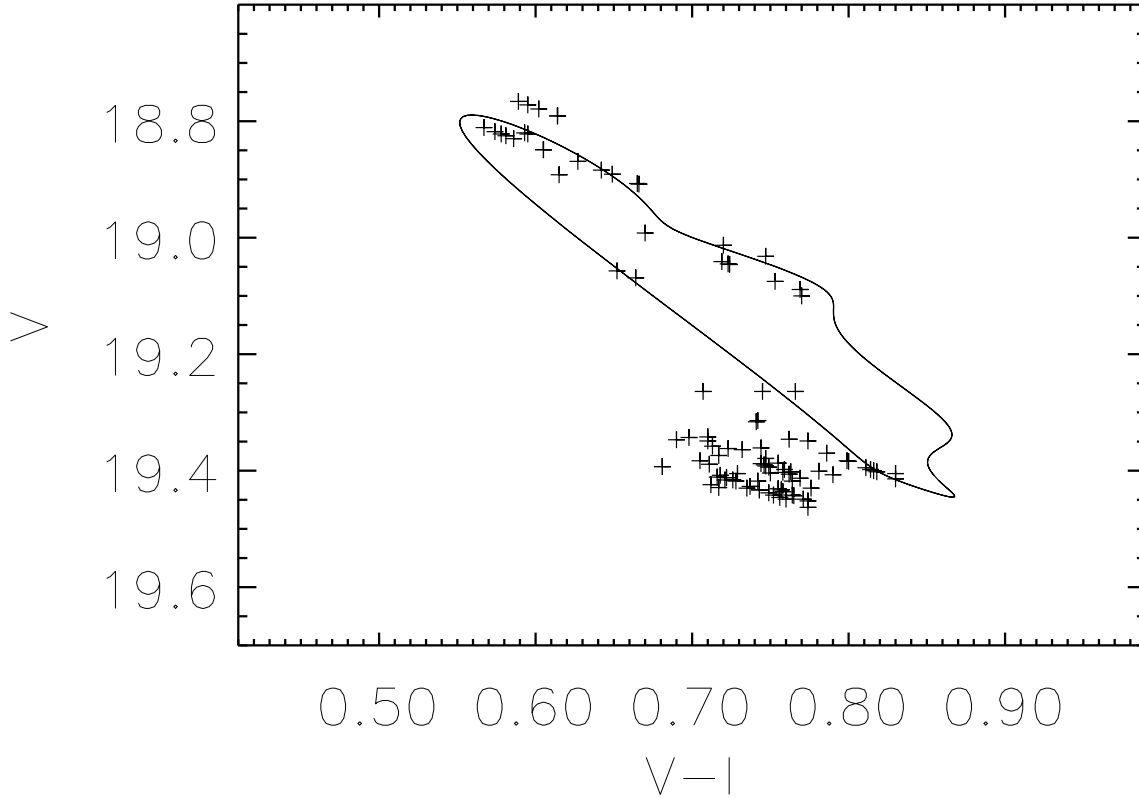
V7184 D31B

Fig. 8.— The color-magnitude loop of the M31 Cepheid D31B V7184 from our DIRECT observations (crosses), projecting a variation in luminosity which is tightly correlated with the temperature variation. For a single Cepheid the loop is traversed in a clockwise direction, as shown by the model (solid). The DIRECT observations of V7184 include the constant flux of two unresolved blue B-stars − the effect on the loop is dramatic despite gaps in the phase coverage of the light curves. Notice that when the Cepheid is bright (upper left part) it is less affected by the blending and follows its loop as expected.

one of the galaxies observed by the HST Key Project on the Extragalactic Distance Scale, NGC 2541 (Ferrarese et al. 1998), several criteria were used to reject Cepheids which may suffer from crowding. We have applied them to our sample of 22 Cepheids to estimate their effectiveness in detecting blending. As we discussed already in §1, blending and crowding are different phenomena, and judging from §5 they do not seem much correlated in M31 either, but it would be helpful if these criteria could detect blending.

One of the proposed tests (Ferrarese et al. 1998) involves identifying Cepheids that have companions not resolved by profile photometry programs by looking at their photometric errors. The underlying idea is that the photometric error would be higher than in case of an isolated star of the same magnitude due to a poorer PSF fit resulting from the unresolved companion. We have
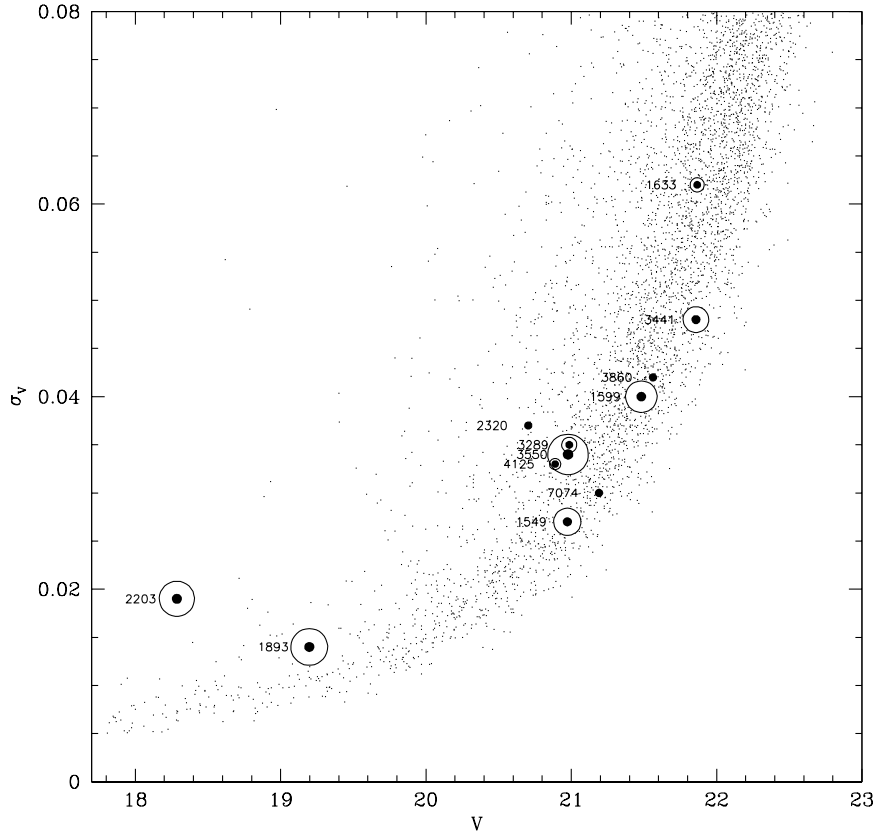
Fig. 9.— The ALLSTAR photometric error σ_V plotted as a function of the ALLSTAR V magnitude. The field F Cepheids are denoted by solid dots surrounded by circles with their size proportional to S_V (no outside circle means $S_V = 0$). The V magnitudes and the errors are taken from the field F template image (FWHM$\sim 1''$), as are the stars plotted in the background.

constructed diagrams showing the ALLSTAR photometric error σ_V as a function of the ALLSTAR V magnitude, similar to the one presented in Fig. 8 of Ferrarese et al. (1998). The diagram for field F is shown in Figure 9. The Cepheids are plotted as solid dots surrounded by circles with their size proportional to the amount of blending S_V (no outside circle means $S_V = 0$). The V magnitudes and the errors are taken from the field F template image (FWHM$\sim 1''$), as are the stars plotted in the background.

Upon examining Figure 9 it is apparent that the photometric errors σ_V do not show a correlation with the amount of light coming from companions S_V. One such case is V2320 D31F which is an unblended star with an error almost twice as large than most stars of similar magnitude. Another example is V3289 D31F with $S_V = 0.11$, which has a photometric error larger than two other, more blended Cepheids of similar V magnitude: V1549 D31F with $S_V = 0.28$ and V3550 D31F with $S_V = 0.47$. Most of the Cepheids lie within the most densely populated areas of the diagram, with V2320 D31F and V2203 D31F being the most clear outliers. A similar photometric error distribution, uncorrelated with S_V, is also seen in fields B and C. In conclusion,

the presence of close companions did not manifest itself in the form of a poorer PSF fit and, hence, a larger photometric error in the studied sample. Another fact which should be kept in mind is that our ground-based PSF is much better sampled than the *HST* PSF (comparing to the respective FWHMs), thus it should be more sensitive to any deformations resulting from the superposition of two or more stars.

Another proposed method of rejecting blended Cepheids is to remove all stars having companions contributing more than 50% of the total light within a radius of two pixels. Taking into account the fact that the two pixels on the *HST* WF chips correspond to twice the FWHM, we have conducted a similar test on our ground-based V template data for the Cepheids. Only one of our Cepheids, V5646 D31B with $S_V = 0.05$ would be rejected from our sample on the basis of this criterion. This test also failed to identify the blended Cepheids in our sample.

A third proposed test for blending is to check if the Cepheid lies on the instability strip in the CMD. The usual color range spanned by the final sample of Cepheids discovered with *HST* is about one magnitude, for example $0.4 \leq V - I \leq 1.4$ in NGC 2541 (Ferrarese et al. 1998), $0.4 \leq V - I \leq 1.5$ in NGC 4639 (Saha et al. 1997), $0.6 \leq V - I \leq 1.5$ in NGC 4535 (Macri et al. 1999). The examination of a ground-based CMD for the 12 field F Cepheids yields a $V - I$ color span of also about one magnitude ($0.6 \leq V - I \leq 1.6$). No clear correlation of the color with the S_V of the Cepheid is seen in the diagram, as unblended Cepheids also exhibit a large color scatter, from $V - I = 0.73$ for V2320 D31F to 1.59 for V3860 D31F, most likely due to differential reddening.

In the case of our sample of 22 Cepheids, the tests were not successful in rejecting the blends. These tests may be helpful in some cases of blending, when the two stars are almost resolved or when the companion has a larger flux contribution than the maximum value of $S_V = 0.47$ present in our sample. But a contamination of $S_V = 0.47$ has a large impact on the photometry of the Cepheid, which actually would be dimmer by almost one third from the measured brightness.

8.   Conclusions

For our sample of 22 Cepheids with both ground-based and *HST* data, we find that the mean V-band flux contribution from companions unresolved in the ground-based images, $\langle S_V \rangle$, is about 19% of the flux of the Cepheid, while the median S_V is 12%. This shows that blending could potentially be a substantial source of error in the Cepheid distance scale, as the distance derived from our ground-based photometry for this admittedly small Cepheid sample would be systematically underestimated by $\sim 9\%$ (for the mean S_V) or $\sim 6\%$ (for the median S_V). This is to be compared to the current Cepheid distance to M31 (which is subject to the LMC distance uncertainty) of $R_{M31} = 770 \pm 25\ kpc$ (Freedman & Madore 1990; Kaluzny et al. 1998; Sasselov et al. 1998). The Cepheid photometry by Freedman & Madore (1990) was from the Canada-France-Hawaii telescope (average seeing $1.0''$, Freedman, Wilson, & Madore 1991). Our
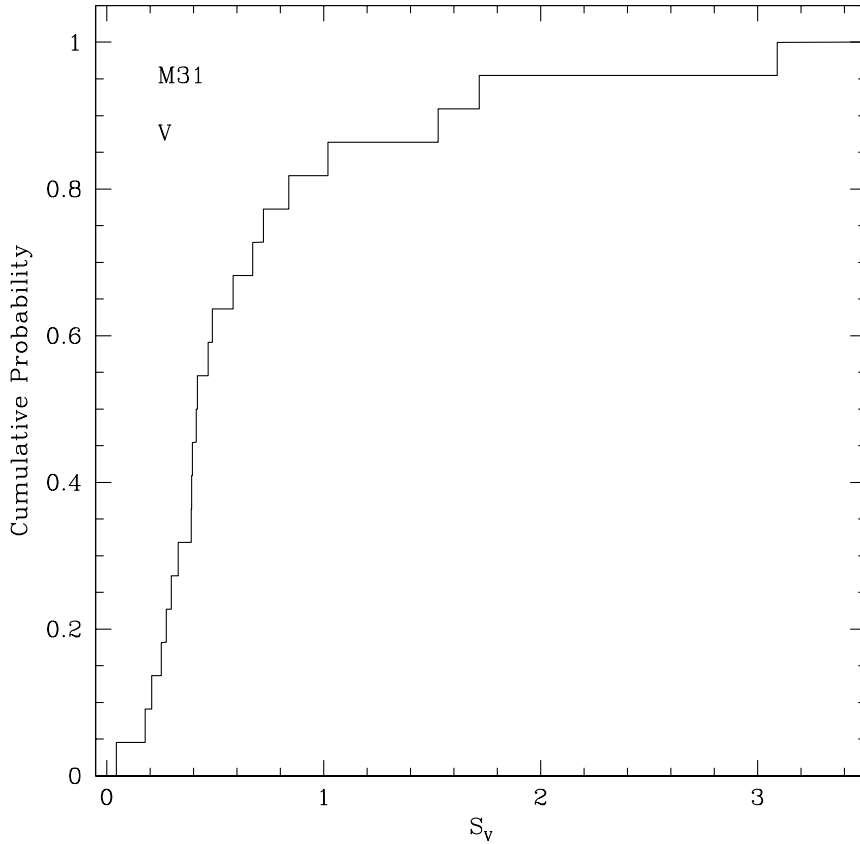
Fig. 10.— The cumulative probability distribution of S_V within a diameter of $3.2''$ of M31 Cepheids with *HST* data, similar to that of one WF pixel $(0.1'')$ at 25 Mpc.

findings of blending here require that these distance estimates to M31 be corrected upward by about 9%.

Blending becomes even more severe when we consider galaxies at a distance of 25 Mpc, i.e. at the edge of what can be currently observed with *HST*. The $0.1''$ FWHM on the WF chips of the WFPC2 camera would span a linear distance of $\sim 12\ pc$ in such a galaxy, which corresponds to $3.2''$ at the distance of M31. In order to obtain an estimate as to the degree of contamination caused by blending at a distance of 25 Mpc, we have summed the contributions of all Cepheid companions within a diameter of $3.2''$ in our *HST* data for M31. The result is presented in Figure 10 in the form of a cumulative probability distribution of S_V. The diagram shows that 50% of our Cepheids have $S_V > 0.4$, though some of the Cepheids with a very high degree of contamination would probably elude detection. This indicates that blending will very likely introduce a significant contamination to Cepheid photometry at such distances and resolution.

As the result of blending with other unresolved stars, the Cepheids appear brighter than they really are when observed in distant galaxies with *HST*. As we compare them with mostly unblended LMC Cepheids, this leads to systematically low distances to galaxies observed with the

HST, and therefore to systematically high estimates of H_0. The sign of the blending effect on the H_0 is opposite to that caused by the lower LMC distance (e.g. Udalski 1998; Stanek et al. 2000) and might be of comparable value, as discussed in this paper. It should be stressed that blending is a factor which contributes in only one direction, and therefore it will not average out when a large sample of galaxies is considered.

One obvious solution to the problem of blending would be to obtain data with better resolution. Such an opportunity will be available after the launch of the Next Generation Space Telescope, scheduled for 2008. An alternative approach would be to determine the amount and color of flux contamination for the Cepheids by the analysis of their light curves and/or color-color loops. The requirement, however, is to have good quality, well-sampled light curves in at least two bands, which is not the case for *HST* Cepheids. However, even with our good light curves it is difficult to detect Cepheids with blending of $S_V < 0.20$.

It must be stressed that the images taken with the *HST* WFPC2 camera, despite having a resolution > 10 times better than our ground-based images (FWHM ~ 0.4 *pc* vs. 5 *pc*), will still leave some blends unresolved, including physical companions (e.g. Evans 1992). Thus, the *V*-band flux contribution from Cepheid companions derived in this paper sets only the lower limit on the true influence of blending on the Cepheid photometry.

REFERENCES

DeYoreo, J. J., & Karp, A. H. 1979, ApJ, 232, 205

Evans, N. R. 1992, ApJ, 389, 657

Evans, N. R. & Udalski, A. 1994, AJ, 108, 653

Fernie, J. D. 1964, ApJ, 140, 699

Ferrarese, L. et al. 1998, ApJ, 507, 655

Ferrarese, L. et al. 2000, ApJ, 529, 745

Freedman, W. L., & Madore, B. F. 1990, ApJ, 365, 186

Freedman, W. L., Wilson, C., & Madore, B. F. 1991, ApJ, 372, 455

Harris, J., & Zaritsky, D. 1999, AJ, 117, 2831

Holland, S. 1998, AJ, 115, 1916

Holtzman, J. et al. 1995, PASP, 107, 156

Jha, S., et al. 1999, ApJS, 125, 73

Kaluzny, J., Stanek, K. Z., Krockenberger, M., Sasselov, D. D., Tonry, J. L., & Mateo, M. 1998, AJ, 115, 1016 (Paper I)

Kaluzny, J., Mochejska, B. J., Stanek, K. Z., Krockenberger, M., Sasselov, D. D., Tonry, J. L., & Mateo, M. 1999, AJ, 118, 346 (Paper IV)

Kennicutt, R. C., et al. 1998, ApJ, 498, 181

Kochanek, C. S. 1997, ApJ, 491, 13

Macri, L. M. et al. 1999, ApJ, 521, 155

Madore, B. F. 1977, MNRAS, 178, 505

Madore, B. F. 1985, ApJ, 298, 340

Mink, D. J. 1997, in ASP Conf. Ser. 125, Astronomical Data Analysis Software and Systems VI, eds. G. Hunt & H. E. Payne (San Francisco: ASP), 249

Mink, D. J. 1999, in ASP Conf. Ser. 172, Astronomical Data Analysis Software and Systems VIII, eds. D. M. Mehringer, R. L. Plante & D. A. Roberts (San Francisco: ASP), 498

Mochejska, B. J., Kaluzny, J., Stanek, K. Z., Krockenberger, M., Sasselov, D. D., 1999, AJ, 118, 2211 (Paper V)

Mochejska, B. J., Macri, L. M., Sasselov, D. D., & Stanek, K. Z. 2000, in preparation

Monet, D., et al. 1996, USNO-SA2.0, (U.S. Naval Observatory, Washington DC)

Moffett, T. J., & Barnes, T. G. 1986, ApJ, 304, 607

Mould, R. R., et al. 2000, ApJ, 529, 786

Pel, J. W., van Genderen, A. M., & Lub, J. 1981, A&A, 99, L1

Rebel, B. J. 1998, undergraduate thesis

Saha, A., Sandage, A., Labhardt, L., Tammann, G. A., Macchetto, F. D., Panagia, N., 1997 ApJ, 486, 1

Saha, A., Sandage, A., Tammann, G. A., Labhardt, L., Macchetto, F. D., Panagia, N. 1999, ApJ, 522, 802

Sasselov, D. D., et al. 1997, A&A, 324, 471

Sasselov, D. D., Krockenberger, M., Stanek, K. Z., Kaluzny, J., Beaulieu, J. P., Tonry, J. L., & Mateo, M. 1998, BAAS, 193, 106.01

Stanek, K. Z., & Garnavich, P. M. 1998, ApJ, 503, L131

Stanek, K. Z., Kaluzny, J., Krockenberger, M., Sasselov, D. D., Tonry, J. L., & Mateo, M. 1998, AJ, 115, 1894 (Paper II)

Stanek, K. Z., Kaluzny, J., Krockenberger, M., Sasselov, D. D., Tonry, J. L., & Mateo, M. 1999, AJ, 117, 2810 (Paper III)

Stanek, K. Z., Kaluzny, J., Wysocka, A., & Thompson, I., 2000, AcA, submitted (astro-ph/9908041)

Stetson, P. B. et al. 1998, ApJ, 508, 491

Stetson, P. B. 1987, PASP, 99 191

Stetson, P. B. 1992, in ASP Conf. Ser. 25, Astrophysical Data Analysis Software and Systems I, eds. D. M. Worrall, C. Bimesderfer, & J. Barnes (San Francisco: ASP), 297

Stobie, R. S. 1970, MNRAS, 148, 1

Udalski, A. 1998, AcA, 48, 383